

# Directed motion of $C_{60}$ on a graphene sheet subjected to a temperature gradient

A. Lohrasebi<sup>1</sup>, M. Neek-Amal<sup>2</sup>, and M. R. Ejtehadi<sup>3</sup>

<sup>1</sup>Department of Physics, University of Isfahan, Isfahan, Iran.

<sup>2</sup>Department of Physics, Shahid Rajaei Teacher Training University, Lavizan, Tehran 16788, Iran.

<sup>3</sup> Department of Physics, Sharif University of Technology, Tehran P.O.Box 1155-9161, Iran.

April 11, 2021

## Abstract

Nonequilibrium molecular dynamics simulations is used to study the motion of a  $C_{60}$  molecule on a graphene sheet subjected to a temperature gradient. The  $C_{60}$  molecule is actuated and moves along the system while it just randomly dances along the perpendicular direction. Increasing the temperature gradient increases the directed velocity of  $C_{60}$ . It is found that the free energy decreases as the  $C_{60}$  molecule moves toward the cold end. The driving mechanism based on the temperature gradient suggests the construction of nanoscale graphene-based motors.

## 1 Introduction

Since graphene has been discovered [1], many properties of this two-dimensional material have been studied both experimentally [2] and theoretically [3, 4]. In a recent experimental research the dynamic of light atoms deposited on a single-layer graphene has been studied by the mean of transmission electron microscopy (TEM) technic [5]. The two-dimensional structure of graphene suggests the possibility of motion with just two degrees of freedom. The free energy surface for a particle moving above a graphene sheet explains different motion-related phenomena at nanoscale as well as the various directed motions on the carbon nanotube-based motors [6, 7].

A net motion can be obtained from a nanoscale system subjected to a thermal gradient [8, 9]. Recently the motion of an experimentally designed nanoscale motor consisting of a capsule-like carbon nanotube inside a host carbon nanotube has been explained successfully with molecular dynamics (MD) simulations [10]. The capsule travels back and forth between both ends of the host carbon nanotube along the axial direction. Barreiro *et al.* have designed an

artificial nanofabricated motor in which one short carbon nanotube travels relative to another coaxial carbon nanotube [7]. This motion is actuated by a thermal gradient as high as  $1 \text{ K nm}^{-1}$  applied to the ends of the coaxial carbon nanotubes.

Since graphene has a very high thermal conductivity ( $3000\text{-}5000 \text{ W K}^{-1} \text{ m}^{-1}$  [11, 12]), as high as diamond and carbon nanotubes [13, 14, 15, 16], it is a good candidate for heat transferring designs in nano-electromechanical systems. Because of strong covalent bonds in graphene, thermal lattice conduction dominates the electrons contribution [11]. Recently Yang *et al.* [17] have studied the thermal conductivity and thermal rectification of trapezoidal and rectangular graphene nanoribbons and found a significant thermal rectification effect in asymmetric graphene ribbons [17].

Here we study the motion of a nanoscale object, e.g.  $C_{60}$ , on a graphene sheet, in the presence of a temperature gradient. We show that the graphene is a good two-dimensional substrate for thermal actuation due to its high thermal conductivity, however as it is expected, in the absence of a thermal gradient, the  $C_{60}$  molecule randomly diffuses on the graphene sheet [6]. The average velocity along the temperature gradient direction and the free energy change throughout the system are calculated.

This paper is organized as follows. In Sec. 2 we will introduce the atomistic model and the simulation method. Sec. 3 contains the main results including those for the produced temperature gradient, the trajectory of the  $C_{60}$  molecule over the graphene sheet and the free energy change. A brief summary and conclusions are included in Sec. 4.

## 2 The model and method

The system was composed of a graphene sheet as a substrate, with dimensions  $L_x \times L_y = 70 \times 5 \text{ nm}^2$  and a  $C_{60}$  molecule above the sheet. The graphene sheet with  $N = 14\,400$  carbon atoms was divided into 12 equal rectangular segments. Each segment with  $N_l = 1200$  carbon atoms was arranged in 40 atomic rows (along armchair or  $x$ -direction). Each row has 30 atoms which were arranged along zigzag direction. The system was equilibrated for 300 ps at  $T = 300 \text{ K}$  before the temperature gradient was applied. Once the system was equilibrated, the first (hot spot) and last (cold end) segments of the graphene sheet were kept at  $T_h$  and  $T_c$ , respectively. A temperature gradient between the two ends was then produced, i.e.  $(T_h - T_c)/L_x$  (top panel of Fig. 1). To make the model more efficient and prevent crumpling (see Fig. 2(a)) of the ends, we fixed the  $z$ -components of the first atomic row in the first segment and the last row of the last segment (see Fig. 2(b)).

We carried out MD simulations employing two types of the interatomic potentials: 1) the covalent bonds between the carbon atoms in the graphene sheet and in the  $C_{60}$  molecule are described by Brenner potential [18] and 2) the non-bonded Van der Waals interactions between the graphene atoms and those of the  $C_{60}$  molecule. Brenner potential has been parameterized to model  $sp^2$  covalent

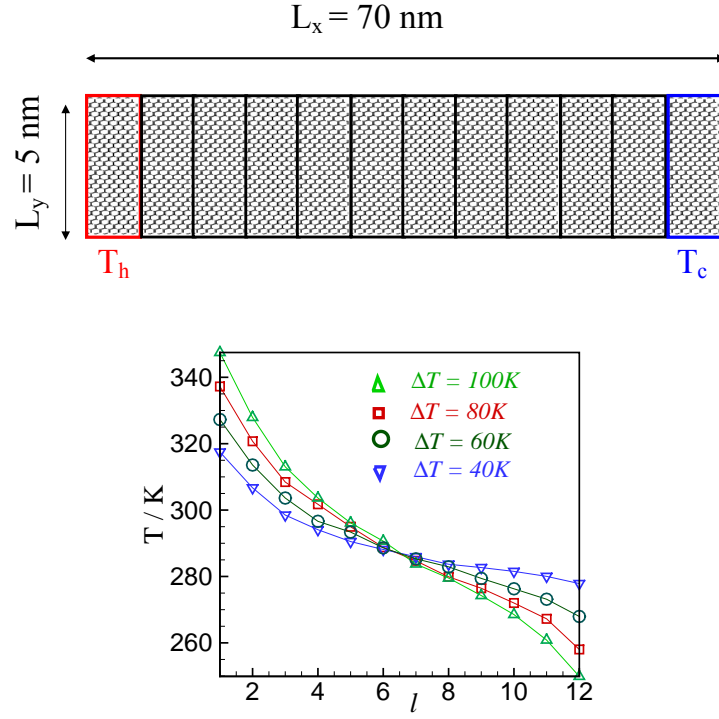


Figure 1: (Color online) Top: The model which shows applied temperature gradient along  $x$ -direction. Bottom: Produced four temperature gradients after 450 ps of a nonequilibrium molecular dynamics simulation. Delta symbols are related to  $\Delta T = 100 \text{ K}$ , and for square symbols  $\Delta T = 80 \text{ K}$ , circle symbols  $\Delta T = 60 \text{ K}$  and for gradient symbols  $\Delta T = 40 \text{ K}$ , respectively.

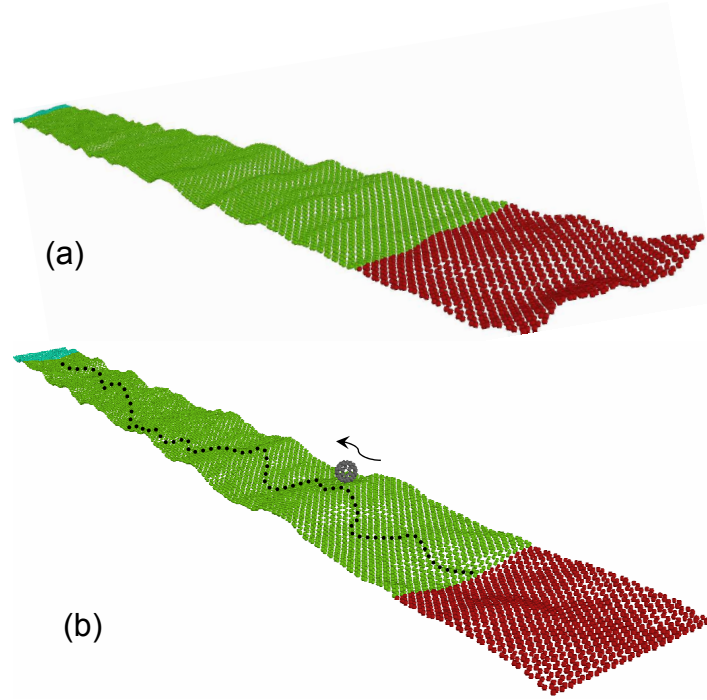


Figure 2: (Color online) (a) A snapshot of a not-constrained system shows the effect of the ends crumpling. (b) Fixing  $z$ -components of the atoms at the first and last rows (see the text) prevents the crumpling. The black dots show a typical trajectory of the motion of a  $C_{60}$  molecule over the graphene sheet from the hot spot toward the cold spot.

bonds in the graphene, carbon nanotube and  $C_{60}$  structures. For the non-bonded potential a Lennard-Jones (LJ) potential gives reasonable results [19]. Here we choose the LJ parameters as  $\epsilon = 2.413 \text{ meV}$  and  $\sigma = 3.4 \text{ \AA}$  [20] which represent the depth and range of the LJ potential energy, respectively. Note that the LJ potential is a simple and commonly used potential for modeling the interaction between carbon nanostructures [21, 22]. The equations of motion were integrated using a velocity-Verlet algorithm with a time step  $\Delta t = 0.5 \text{ fs}$ . The temperature of the hot end ( $T_h$ ) and the cold end ( $T_c$ ) were held constant by a Nosé-Hoover thermostat. The temperature of the inner segments were not controlled by the thermostat. Periodic boundary condition was applied only in the  $y$ -direction. Due to the applied temperature gradient, the system can no longer be described by equilibrium methods and we shall thus employ nonequilibrium molecular dynamics simulations. A temperature gradient were produced across the system during 450 ps and a stationary state was established. The  $C_{60}$  molecule was put above the second segment at  $z_{cm} = 8 \text{ \AA}$  (here index  $cm$  refer to the center of mass). During the production runs of 750 ps both the  $x$  and  $y$  positions of the center of mass of the  $C_{60}$  molecule were recorded. Moreover the temperature of each segment was calculated by measuring the total kinetic energy of that segment. In our simulations a typical value for the relative standard deviation of the total energy of the extended system is about  $3.5 \times 10^{-5}$ . A full simulation run takes about 50 h CPU time on a 3.2 GHz Pentium IV processor with 4 GB RAM.

In order to compute the change in the free energy, one can employ the commonly used thermodynamic integration and perturbation methods [23]. A good estimation for the absolute value of the free energy requires sampling the whole phase space which is not feasible. Jarzynski's method removes this difficulty for nonequilibrium simulations [24]. There is an equality between the change of the free energy  $F$  and the work  $W$  applied on the system (here the  $C_{60}$  molecule) [24]

$$\Delta F = -\beta^{-1} \ln \overline{\exp(-\beta W)}, \quad (1)$$

where  $\beta = 1/k_B T$  ( $T$  is the temperature in each segment), and the average is taken over different configurations with different initial conditions. In fact, Eq. (1) connects the change of the free energy (between two equilibrium state) and the applied work on the system in a nonequilibrium process.

### 3 Results and discussion

#### 3.1 Producing temperature gradient

The temperature profiles for different temperature gradients with  $\Delta T = 40, 60, 80, 100 \text{ K}$  are shown in Fig. 1 (bottom panel). In this figure, the local temperatures of each segment which were obtained by averaging over 500 data are indicated by symbols. Corresponding error bars indicate the statistical errors and are in the range 4-6 K. Notice that the temperature profiles are nonlinear which is a commonly observed behavior in nonequilibrium molecular dynamics simulation

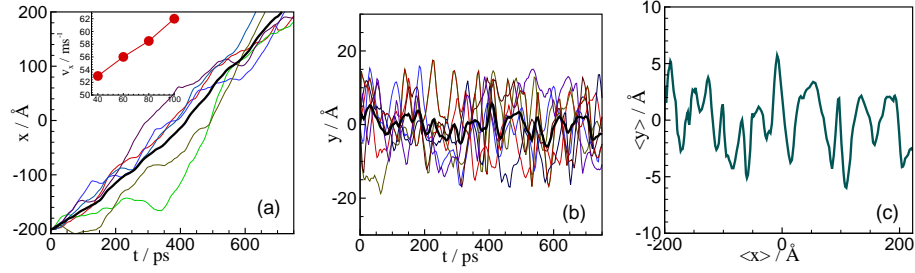


Figure 3: (Color online) (a, b) Time series of  $x$  and  $y$  components of the center of mass of a  $C_{60}$  molecule over a monolayer graphene subjected to a temperature gradient. Thick curves show the average curves. The inset shows the variation of the velocity versus temperature gradient. (c) The trajectory of the motion of a  $C_{60}$  molecule (in  $x - y$  plane) moving over the monolayer graphene, averaged over six simulations with different initial conditions.

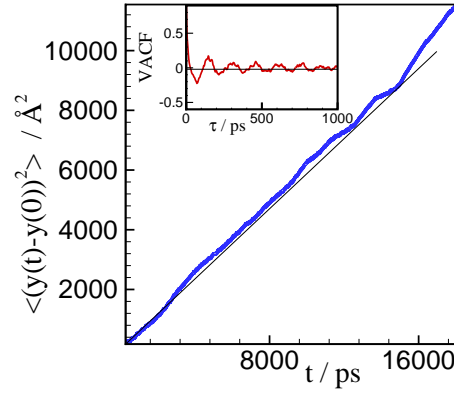


Figure 4: (Color online) Mean square displacement for  $y$ -component of the center of mass of  $C_{60}$  molecule over the graphene. The inset shows the velocity autocorrelation function for the  $y$ -component of the motion as a function of time.

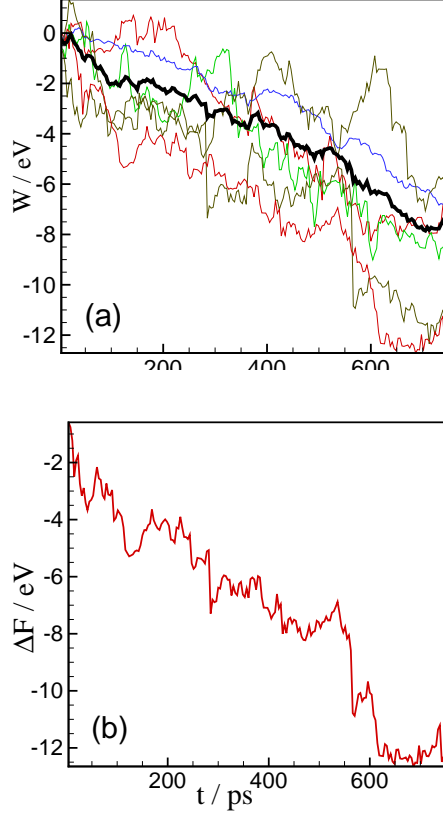


Figure 5: (Color online) (a) Total work performed on C<sub>60</sub> molecules and (b) the change of free energy during C<sub>60</sub> motion from the hot end to the cold end. The thick curve is the average over six simulations with different initial conditions.

of thermal conductivity [14, 15, 16]. It is a consequence of the strong phonon scattering caused by the heat source or heat sink and can be explained by partly diffusive and partly ballistic energy transport along the system [14, 25]. Also, ripples in the graphene (Fig. 2(b)) are the other important source for phonon scattering [26, 27]. Therefore, these mechanisms cause a non-linear temperature profile in the middle segments.

### 3.2 Trajectory in the $x - y$ plane

The graphene ribbon is a two-dimensional way for the motion of the C<sub>60</sub> molecule along it. C<sub>60</sub> attempts to find its equilibrium state and looks for the local minimum of the free energy. In other words, in the presence of a temperature gradient, the phonon waves created in the hot spot travel through the system,

interact and transfer momentum to the  $C_{60}$  molecule which results a net motion [7]. The time series for the  $x$  and  $y$  coordinates, separately, are shown in Figs. 3(a,b). The trajectories of the six  $C_{60}$  molecules (from the six different simulations) in  $x-y$  plane over a time interval of 750 ps are depicted in Fig. 3(c). In all three cases the thick curve is the average of the six others.

The motion along the  $x$ -direction is almost a linear uniform motion with velocities  $v_x = 53, 56, 59$  and  $63$  m/s for  $\Delta T = 40, 60, 80, 100$  K respectively (see inset of Fig. 3(a)). There are two computational methods that can be used to show that the motion along the  $y$ -direction is diffusive (Fig. 3(c)). First, one can use the Einstein relation to find the diffusion constant  $D_y$  by measuring the slope of the mean square displacement (MSD) of the  $y$ -components of the position, i.e.  $\langle (y(t) - y(0))^2 \rangle$ . To show that the motion along the  $y$ -direction is driftless, we look at the MSD of  $y$ -component of the position of the  $C_{60}$  molecule. For a driftless motion the MSD should grows linearly with time, i.e.  $\langle (y(t) - y(0))^2 \rangle = 2D_y t$ . We depict the MSD in Fig. 4 for a long time simulation. As we see from this figure the slope of the MSD is almost one (after equilibration) which is a signature of diffusive regime. Alternatively one can use the Green-Kubo relation which makes use of the velocity autocovariance function (VACF). More specifically, one can take the integral over the autocovariance of the  $y$ -components of the position of the velocity of  $C_{60}$  as  $D_y = \int_0^\infty \langle v_y(0)v_y(\tau) \rangle d\tau$ , which gives the diffusion constant of random walk motion along the  $y$ -axis. The inset of Fig. 4 shows the VACF versus time. We have tested both methods in order to compute  $D_y$ . The result for the diffusion constant is about  $4 \times 10^{-9} \text{ m}^2/\text{s}$ .

The directed motion resulted from the temperature gradient along the graphene sheet, provides a nanoscale motor for the material transferring. Notice that in the absence of temperature gradient, when the system is equilibrated at  $T = 300$  K, we found a diffusive motion on the graphene sheet [6].

### 3.3 Free energy reduction

Figures 5(a,b) show the variation of the total work and the changes in the free energy with time, respectively. The  $C_{60}$  loses on average almost 12 eV of free energy after 750 ps during the motion towards the cooler region. Note that here, the condition  $\overline{W} > \Delta F$  is always satisfied which is a well known criterion for a nonequilibrium (irreversible) thermodynamics evolution [24]. This method for calculating the change of the free energy is a well known method in computational soft condensed matter [28] but it turns out to be useful also for studying various physical properties of graphene, particularly investigating the stability of new designs for nanoscale molecular devices as studied here.

## 4 Conclusions

In summary,  $C_{60}$  moves directly toward the cold end of the graphene sheet when a temperature gradient is applied along armchair direction. It is found that the



lateral motion (along zigzag direction) is a diffusive motion. The reduction of the free energy of the system along the molecule motion is an indicative of the drifted motion. Comparing the free energy difference with the work performed on  $C_{60}$  shows that the process is indeed thermodynamically irreversible. The proposed mechanism for driving nanoparticles on a graphene sheet may be used in the design of novel nanoscale motors.

## 5 Acknowledgment

We gratefully acknowledge valuable comments from Hamid Reza Sepangi and Ali Naji.

## References

- [1] K. S. Novoselov, A. K. Geim, S. V. Morozov, D. Jiang, Y. Zhang, S. V. Dubonos, I. V. Grigorieva, and A. A. Firsov, *Science* **306**, 666 (2004) .
- [2] A. K. Geim, and K. S. Novoselov, *Nature Mater.* **6**, 183 (2007).
- [3] A. K. Geim and A. H. MacDonald, *Phys. Today* **60**, 35 (2007).
- [4] A. H. Castro Neto, F. Guinea, N. M. Peres, K. S. Novoselov, and A. K. Geim, *Rev. Mod. Phys.* **81**, 109 (2009).
- [5] J. C. Meyer, C. O. Girit, M. F. Crommie and A. Zettl, *Nature* **454**, 319-322 (2008).
- [6] M. Neek-Amal, N. Abedpour, S. N. Rasuli, A. Naji, and M. R. Ejtehadi, *Phys. Rev. E*, **82**, 051605 (2010).
- [7] A. Barreiro, R. Rurali, E.R. Hernandez, J. Moser, T. Pichler, L. Forro, and A. Bachtold, *Science* **320**, 775 (2008).
- [8] P. A. E. Schoen, J. H. Walther, S. Arcidiacono, D. Poulikakos, P. Koumoutsakos, *Nano Lett.* **6**, 1910 (2006).
- [9] P. A. E. Schoen, J. H. Walther, D. Poulikakos, P. Koumoutsakos, *Appl. Phys. Lett.* **90**, 253116 (2007).
- [10] H. Somada, K. Hirahara, S. Akita, and Y. Nakayama, *Nano Lett.* **9**, 62 (2009).
- [11] A. A. Balandin, S. Ghosh, W. Bao, I. Calizo, D. Teweldebrhan, F. Miao, C. N. Lau, *Nano Lett.* **8**, 902 (2008).
- [12] S. Ghosh, I. Calizo, D. Teweldebrhan, E. P. Pokatilov, D. L. Nika, A. A. Balandin, W. Bao, F. Miao, C. N. Lau, *Appl. Phys. Lett.* **92**, 151911 (2008).
- [13] S. Berber, Y-K Kwon, and D. Tomanek, *Phys. Rev. Lett.* **84**, 4613 (2000).

- [14] P. K. Schelling, S. R. Phillpot, and P. Keblinski, Phys. Rev. B. **65**, 144306 (2002).
- [15] E. Gonzalez Noya, D. Srivastava, Leonid A. Chernozatonskii, M. Menon, Phys. Rev. B. **70**, 115416 (2004).
- [16] M. A. Osman and D. Srivastava, Nanotechnology, **12** 21 (2001).
- [17] N. Yang, G. Zhang, and B. Li, Appl. Phys. Lett. **95**, 033107 (2009).
- [18] D. W. Brenner, Phys. Rev. B. **42**, 9458 (1990).
- [19] H. Ulbricht, G. Moos, and T. Hertel, Phys Rev Lett. **7**, 095501 (2003).
- [20] G. Stan, M. J. Bojan, S. Curtarolo, S. M. Gatica, and M. W. Cole, Phys. Rev. B **62**, 2173 (2000).
- [21] P. A. Gravil, M. Devel, Ph. Lambin, X. Bouju, Ch. Girard, and A. A. Lucas, Phys. Rev. B **53**, 1622 (1996).
- [22] A. N. Kolmogorov, and V. H. Crespi, Phys. Rev. Lett **85**, 4727 (2000).
- [23] F. Colonna, J. H. Los, A. Fasolino, and E. J. Meijer, Phys. Rev. B **80**, 134103 (2009).
- [24] C. Jarzynski, Phys. Rev. Lett **78**, 2690 (1997).
- [25] C. Oligschleger and J. C. Schon, Phys. Rev. B **59**, 4125 (1999).
- [26] K. V. Zakharchenko, M. I. Katsnelson, and A. Fasolino, Phys. Rev. Lett **102**, 046808 (2009).
- [27] N. Abedpour, M. Neek-Amal, R. Asgari, F. Shahbazi, N. Nafari, and M. R. Tabar, Phys. Rev. B **76**, 195407 (2007).
- [28] H. Xiong, A. Crespo1, M. Marti, D. Estrin, and A. E. Roitberg, Theor. Chem. Acc. **116**, 338 (2002).